

Introductory Raman spectroscopy

Author(s) Ferraro, John R. ; Nakamoto, Kazuo ; Brown, Chris W. ; ebrary, Inc
Imprint Amsterdam ; Boston : Academic Press, c2003
Extent xiii, 434 p.
Topic QC
Subject(s) Raman spectroscopy
Language English
ISBN 0122541057
Permalink <http://books.scholarsportal.info/viewdoc.html?id=406107>
Pages 1 to 45



INTRODUCTORY RAMAN SPECTROSCOPY

2nd Edition

John R. Ferraro &
Kazuo Nakamoto

INTRODUCTORY RAMAN SPECTROSCOPY

SECOND EDITION

This Page Intentionally Left Blank

INTRODUCTORY RAMAN SPECTROSCOPY

SECOND EDITION

John R. Ferraro

*Argonne National Laboratory
Argonne, Illinois*

Kazuo Nakamoto

*Marquette University
Milwaukee, Wisconsin*

Chris W. Brown

*University of Rhode Island
Kingston, Rhode Island*



ACADEMIC PRESS

An imprint of Elsevier Science

Amsterdam Boston London New York Oxford Paris
San Diego San Francisco Singapore Sydney Tokyo

COVER FIGURE: Raman spectra of two polymorphs of Cimetidine are shown on the cover. Cimetidine is a pharmaceutical product that has six polymorphic forms and each form has a distinctive Raman spectrum as shown in Figure 4.25 of Chapter 4 (with permission of Ref. 47). The particular polymorphic or crystalline form of a compound can be very important since the bio-availability and patent positions often depend upon the form. Raman spectra can be used to easily identify the polymorphic form.

This book is printed on acid-free paper.

Copyright 2003, 1994 Elsevier Science (USA)

All rights reserved.

No part of this publication may be reproduced or transmitted in any form or by any means, electronic or mechanical, including photocopy, recording, or any information storage and retrieval system, without permission in writing from the publisher.

Requests for permission to make copies of any part of the work should be mailed to:
Permissions Department, Harcourt, Inc., 6277 Sea Harbor Drive, Orlando, Florida 32887-6777.

Academic Press

An imprint of Elsevier Science

525 B Street, Suite 1900, San Diego, California 92101-4495, USA

<http://www.academicpress.com>

Academic Press

84 Theobald's Road, London WC1X 8RR, UK

<http://www.academicpress.com>

Library of Congress Control Number: 2002100071

International Standard Book Number: 0-12-254105-7

PRINTED IN THE UNITED STATES OF AMERICA

02 03 04 05 06 9 8 7 6 5 4 3 2 1

*The authors wish to dedicate this book to their wives,
Mary Ferraro, Kimiko Nakamoto, and Kathleen Brown.*

This Page Intentionally Left Blank

Contents

Preface to the Second Edition	x
Acknowledgments	xi
Preface to the First Edition	xii
Acknowledgments	xiii
Chapter 1. Basic Theory	1
1.1. Historical Background of Raman Spectroscopy	1
1.2. Energy Units and Molecular Spectra	2
1.3. Vibration of a Diatomic Molecule	7
1.4. Origin of Raman Spectra	13
1.5. Factors Determining Vibrational Frequencies	18
1.6. Vibrations of Polyatomic Molecules	19
1.7. Selection Rules for Infrared and Raman Spectra	22
1.8. Raman versus Infrared Spectroscopy	26
1.9. Depolarization Ratios	27
1.10. The Concept of Symmetry	30
1.11. Point Symmetry Elements	31
1.12. The Character Table	43
1.13. Classification of Normal Vibrations by Symmetry	48
1.14. Symmetry Selection Rules	52
1.15. Resonance Raman Spectra	54
1.16. Space Group Symmetry	61

1.17.	Normal Vibrations in a Crystal	67
1.18.	Selection Rules for Solids (Factor Group)	70
1.19.	Polarized Raman Spectra of Single Crystals	78
1.20.	Normal Coordinate Analysis	79
1.21.	Band Assignments and Isotope Shifts	86
	References	89
	General References	91
Chapter 2.	Instrumentation and Experimental Techniques	95
2.1.	Major Components	95
2.2.	Excitation Sources	96
2.3.	Sample Illumination	103
2.4.	Wavelength Selectors	105
2.5.	Detection	112
2.6.	Instrument Calibration	117
2.7.	Sampling Techniques	123
2.8.	Fluorescence Problems	137
2.9.	Raman Difference Spectroscopy	138
2.10.	Miniature Raman Spectrometers	140
	References	143
	General References	146
Chapter 3.	Special Techniques	147
3.1.	High-Pressure Raman Spectroscopy	147
3.2.	Raman Microscopy	154
3.3.	Surface-Enhanced Raman Spectroscopy (SERS)	161
3.4.	Raman Spectroelectrochemistry	168
3.5.	Time-Resolved Raman (TR ²) Spectroscopy	174
3.6.	Matrix-Isolation Raman Spectroscopy	179
3.7.	2D Correlation Raman Spectroscopy	184
3.8.	Raman Imaging Spectrometry	188
3.9.	Nonlinear Raman Spectroscopy	194
	References	202

Contents	ix
Chapter 4. Materials Applications	207
4.1. Applications to Structural Chemistry	207
4.2. Solid State Applications	237
References	263
Chapter 5. Analytical Chemistry	267
5.1. Preprocessing Spectra	267
5.2. Full-Spectra Processing Methods	277
5.3. Quantitative Analysis	283
5.4. Spectral Searches	285
5.5. Discriminant Analysis	288
References	292
Chapter 6. Biochemical and Medical Applications	295
6.1. Biochemical Applications	296
6.2. Medical Applications	313
References	322
Chapter 7. Industrial, Environmental and Other Applications	325
7.1. Industrial Applications	325
7.2. Environmental Applications	342
7.3. Other Applications	350
References	361
Appendices	363
Index	423

Preface to the Second Edition

The second edition of *Introductory Raman Spectroscopy* treats the subject matter on an introductory level and serves as a guide for newcomers in the field.

Since the first edition of the book, the expansion of Raman spectroscopy as an analytical tool has continued. Thanks to advances in laser sources, detectors, and fiber optics, along with the capability to do imaging Raman spectroscopy, the continued versatility of FT-Raman, and dispersive based CCD Raman spectrometers, progress in Raman spectroscopy has flourished. The technique has moved out of the laboratory and into the workplace. In situ and remote measurements of chemical processes in the plant are becoming routine, even in hazardous environments.

This second edition contains seven chapters. Chapter 1 remains a discussion of basic theory. Chapter 2 expands the discussion on Instrumentation and Experimental Techniques. New discussions on FT-Raman and fiber optics are included. Sampling techniques used to monitor processes in corrosive environments are discussed. Chapter 3 concerns itself with Special Techniques; discussions on 2D correlation Raman spectroscopy and Raman imaging spectroscopy are provided. The new Chapter 4 deals with materials applications in structural chemistry and in solid state. A new section on polymorphs is presented and demonstrates the role of Raman spectroscopy in differentiating between polymorphs, an important industrial problem, particularly in the pharmaceutical field. The new Chapter 5 is based on analytical applications and methods for processing Raman spectral data, a subject that has generated considerable interest in the last ten years. The discussion commences with a general introduction to chemometric processing methods as they apply to Raman spectroscopy; it then proceeds to a discussion of some analytical applications of those methods. The new Chapter 6 presents applications in the field of biochemistry and in the medical field, a very rich and fertile area for Raman spectroscopy. Chapter 7 presents industrial applications, including some new areas such as ore refinement, the lumber/paper industry, natural gas analysis, the pharmaceutical/prescription drug industry, and polymers. The second edition, like the first, contains eight appendices.

With these inclusions, we believe that the book brings the subject of Raman spectroscopy into the new millennium.

Acknowledgments

The authors would like to express their thanks to Prof. Robert A. Condrate of Alfred University, Prof. Roman S. Czernuszewicz of the University of Houston, Dr. Victor A. Maroni of Argonne National Laboratory, and Prof. Masamichi Tsuboi of Iwaki-Meisei University of Japan who made many valuable suggestions. Special thanks are given to Roman S. Czernuszewicz for making drawings for Chapters 1 and 2. Our thanks and appreciation also go to Prof. Hiro-o Hamaguchi of Kanagawa Academy of Science and Technology of Japan and Prof. Akiko Hirakawa of the University of the Air of Japan who gave us permission to reproduce Raman spectra of typical solvents (Appendix 8). Professor Kazuo Nakamoto also extends thanks to Professor Yukihiro Ozaki of Kwansei-Gakuin University in Japan and to Professor Kasem Nithipatikom of the Medical College of Wisconsin for help in writing sections 3.7 and 6.2.4 of the second edition respectively. Professor Chris W. Brown would like to thank Su-Chin Lo of Merck Pharmaceutical Co. for aid in sections dealing with pharmaceuticals and Scott W. Huffman of the National Institute of Health for measuring Raman spectra of peptides. All three authors thank Mrs. Carla Kinney, editor for Academic Press, for her encouragement in the development of the second edition.

2002

John R. Ferraro
Kazuo Nakamoto
Chris W. Brown

Preface to the First Edition

Raman spectroscopy has made remarkable progress in recent years. The synergism that has taken place with the advent of new detectors, Fourier-transform Raman and fiber optics has stimulated renewed interest in the technique. Its use in academia and especially in industry has grown rapidly.

A well-balanced Raman text on an introductory level, which explains basic theory, instrumentation and experimental techniques (including special techniques), and a wide variety of applications (particularly the newer ones) is not available. The authors have attempted to meet this deficiency by writing this book. This book is intended to serve as a guide for beginners.

One problem we had in writing this book concerned itself in how one defines "introductory level." We have made a sincere effort to write this book on our definition of this level, and have kept mathematics at a minimum, albeit giving a logical development of basic theory.

The book consists of Chapters 1 to 4, and appendices. The first chapter deals with basic theory of spectroscopy; the second chapter discusses instrumentation and experimental techniques; the third chapter deals with special techniques; Chapter 4 presents applications of Raman spectroscopy in structural chemistry, biochemistry, biology and medicine, solid-state chemistry and industry. The appendices consist of eight sections. As much as possible, the authors have attempted to include the latest developments.

Acknowledgments

The authors would like to express their thanks to Prof. Robert A. Condrate of Alfred University, Prof. Roman S. Czernuszewicz of the University of Houston, Dr. Victor A. Maroni of Argonne National Laboratory, and Prof. Masamichi Tsuboi of Iwaki-Meisei University of Japan who made many valuable suggestions. Special thanks are given to Roman S. Czernuszewicz for making drawings for Chapters 1 and 2. Our thanks and appreciation also go to Prof. Hiro-o Hamaguchi of Kanagawa Academy of Science and Technology of Japan and Prof. Akiko Hirakawa of the University of the Air of Japan who gave us permission to reproduce Raman spectra of typical solvents (Appendix 8). We would also like to thank Ms. Jane Ellis, Acquisition Editor for Academic Press, Inc., who invited us to write this book and for her encouragement and help throughout the project. Finally, this book could not have been written without the help of many colleagues who allowed us to reproduce figures for publication.

1994

John R. Ferraro
Kazuo Nakamoto

This Page Intentionally Left Blank

Chapter 1

Basic Theory

1.1 Historical Background of Raman Spectroscopy

In 1928, when Sir Chandrasekhra Venkata Raman discovered the phenomenon that bears his name, only crude instrumentation was available. Sir Raman used sunlight as the source and a telescope as the collector; the detector was his eyes. That such a feeble phenomenon as the Raman scattering was detected was indeed remarkable.

Gradually, improvements in the various components of Raman instrumentation took place. Early research was concentrated on the development of better excitation sources. Various lamps of elements were developed (e.g., helium, bismuth, lead, zinc) (1–3). These proved to be unsatisfactory because of low light intensities. Mercury sources were also developed. An early mercury lamp which had been used for other purposes in 1914 by Kerschbaum (1) was developed. In the 1930s mercury lamps suitable for Raman use were designed (2). Hibben (3) developed a mercury burner in 1939, and Spedding and Stamm (4) experimented with a cooled version in 1942. Further progress was made by Rank and McCartney (5) in 1948, who studied mercury burners and their backgrounds. Hilger Co. developed a commercial mercury excitation source system for the Raman instrument, which consisted of four lamps surrounding the Raman tube. Welsh *et al.* (6) introduced a mercury source in 1952, which became known as the Toronto Arc. The lamp consisted of a four-turn helix of Pyrex tubing and was an improvement over the Hilger lamp. Improvements in lamps were made by

Ham and Walsh (7), who described the use of microwave-powered helium, mercury, sodium, rubidium and potassium lamps. Stammreich (8–12) also examined the practicality of using helium, argon, rubidium and cesium lamps for colored materials. In 1962 laser sources were developed for use with Raman spectroscopy (13). Eventually, the Ar^+ (351.1–514.5 nm) and the Kr^+ (337.4–676.4 nm) lasers became available, and more recently the Nd-YAG laser (1,064 nm) has been used for Raman spectroscopy (see Chapter 2, Section 2.2).

Progress occurred in the detection systems for Raman measurements. Whereas original measurements were made using photographic plates with the cumbersome development of photographic plates, photoelectric Raman instrumentation was developed after World War II. The first photoelectric Raman instrument was reported in 1942 by Rank and Wiegand (14), who used a cooled cascade type RCA IP21 detector. The Heigl instrument appeared in 1950 and used a cooled RCA C-7073B photomultiplier. In 1953 Stamm and Salzman (15) reported the development of photoelectric Raman instrumentation using a cooled RCA IP21 photomultiplier tube. The Hilger E612 instrument (16) was also produced at this time, which could be used as a photographic or photoelectric instrument. In the photoelectric mode a photomultiplier was used as the detector. This was followed by the introduction of the Cary Model 81 Raman spectrometer (17). The source used was the 3 kW helical Hg arc of the Toronto type. The instrument employed a twin-grating, twin-slit double monochromator.

Developments in the optical train of Raman instrumentation took place in the early 1960s. It was discovered that a double monochromator removed stray light more efficiently than a single monochromator. Later, a triple monochromator was introduced, which was even more efficient in removing stray light. Holographic gratings appeared in 1968 (17), which added to the efficiency of the collection of Raman scattering in commercial Raman instruments.

These developments in Raman instrumentation brought commercial Raman instruments to the present state of the art of Raman measurements. Now, Raman spectra can also be obtained by Fourier transform (FT) spectroscopy. FT-Raman instruments are being sold by all Fourier transform infrared (FT-IR) instrument makers, either as interfaced units to the FT-IR spectrometer or as dedicated FT-Raman instruments.

1.2 Energy Units and Molecular Spectra

Figure 1-1 illustrates a wave of polarized electromagnetic radiation traveling in the z -direction. It consists of the electric component (x -direction) and magnetic component (y -direction), which are perpendicular to each other.

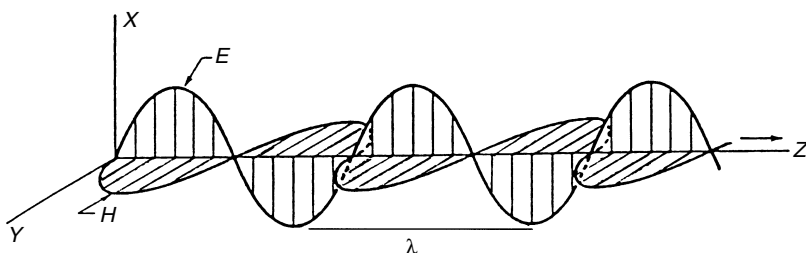


Figure 1-1 Plane-polarized electromagnetic radiation.

Hereafter, we will consider only the former since topics discussed in this book do not involve magnetic phenomena. The electric field strength (E) at a given time (t) is expressed by

$$E = E_0 \cos 2\pi\nu t, \quad (1-1)$$

where E_0 is the amplitude and ν is the frequency of radiation as defined later.

The distance between two points of the same phase in successive waves is called the “wavelength,” λ , which is measured in units such as Å (angstrom), nm (nanometer), $m\mu$ (millimicron), and cm (centimeter). The relationships between these units are:

$$1 \text{ Å} = 10^{-8} \text{ cm} = 10^{-1} \text{ nm} = 10^{-1} m\mu. \quad (1-2)$$

Thus, for example, $4,000 \text{ Å} = 400 \text{ nm} = 400 m\mu$.

The frequency, ν , is the number of waves in the distance light travels in one second. Thus,

$$\nu = \frac{c}{\lambda}, \quad (1-3)$$

where c is the velocity of light (3×10^{10} cm/s). If λ is in the unit of centimeters, its dimension is (cm/s)/(cm) = 1/s. This “reciprocal second” unit is also called the “hertz” (Hz).

The third parameter, which is most common to vibrational spectroscopy, is the “wavenumber,” $\tilde{\nu}$, defined by

$$\tilde{\nu} = \frac{\nu}{c}. \quad (1-4)$$

The difference between ν and $\tilde{\nu}$ is obvious. It has the dimension of (1/s)/(cm/s) = 1/cm. By combining (1-3) and (1-4) we have

$$\tilde{\nu} = \frac{\nu}{c} = \frac{1}{\lambda} (\text{cm}^{-1}). \quad (1-5)$$

Table 1-1 Units Used in Spectroscopy*

10^{12}	tera	T
10^9	giga	G
10^6	mega	M
10^3	kilo	k
10^2	hecto	h
10^1	deca	da
10^{-1}	deci	d
10^{-2}	centi	c
10^{-3}	milli	m
10^{-6}	micro	μ
10^{-9}	nano	n
10^{-12}	pico	p
10^{-15}	femto	f
10^{-18}	atto	a

*Notations: T, G, M, k, h, da, μ , n—Greek;
d, c, m—Latin; p—Spanish; f—Swedish;
a—Danish.

Thus, $4,000 \text{ \AA}$ corresponds to $25 \times 10^3 \text{ cm}^{-1}$, since

$$\tilde{\nu} = \frac{1}{\lambda(\text{cm})} = \frac{1}{4 \times 10^3 \times 10^{-8}} = 25 \times 10^3 \text{ (cm}^{-1}\text{)}.$$

Table 1-1 lists units frequently used in spectroscopy. By combining (1-3) and (1-4), we obtain

$$\nu = \frac{c}{\lambda} = c\tilde{\nu}. \quad (1-6)$$

As shown earlier, the wavenumber ($\tilde{\nu}$) and frequency (ν) are different parameters, yet these two terms are often used interchangeably. Thus, an expression such as “frequency shift of 30 cm^{-1} ” is used conventionally by IR and Raman spectroscopists and we will follow this convention through this book.

If a molecule interacts with an electromagnetic field, a transfer of energy from the field to the molecule can occur only when Bohr’s frequency condition is satisfied. Namely,

$$\Delta E = h\nu = h\frac{c}{\lambda} = hc\tilde{\nu}. \quad (1-7)$$

Here ΔE is the difference in energy between two quantized states, h is Planck’s constant ($6.62 \times 10^{-27} \text{ erg s}$) and c is the velocity of light. Thus, $\tilde{\nu}$ is directly proportional to the energy of transition.

Suppose that

$$\Delta E = E_2 - E_1, \quad (1-8)$$

where E_2 and E_1 are the energies of the excited and ground states, respectively. Then, the molecule “absorbs” ΔE when it is excited from E_1 to E_2 , and “emits” ΔE when it reverts from E_2 to E_1 .

$$\begin{array}{ccc} \overline{\Delta E} & \xrightarrow{\text{absorption}} & E_2 \\ \uparrow & & \\ \overline{E_1} & & \end{array} \quad \begin{array}{ccc} E_2 & \xrightarrow{\Delta E} & \downarrow \text{emission} \\ & & \\ E_1 & & \end{array}$$

Using the relationship given by Eq. (1-7), Eq. (1-8) is written as

$$\Delta E = E_2 - E_1 = hc\tilde{\nu}. \quad (1-9)$$

Since h and c are known constants, ΔE can be expressed in terms of various energy units. Thus, 1 cm^{-1} is equivalent to

$$\begin{aligned} \Delta E &= [6.62 \times 10^{-27} \text{ (erg s)}][3 \times 10^{10} \text{ (cm/s)}][1 \text{ (1/cm)}] \\ &= 1.99 \times 10^{-16} \text{ (erg/molecule)} \\ &= 1.99 \times 10^{-23} \text{ (joule/molecule)} \\ &= 2.86 \text{ (cal/mole)} \\ &= 1.24 \times 10^{-4} \text{ (eV/molecule)} \end{aligned}$$

In the preceding conversions, the following factors were used:

$$\begin{aligned} 1 \text{ (erg/molecule)} &= 2.39 \times 10^{-8} \text{ (cal/molecule)} \\ &= 1 \times 10^{-7} \text{ (joule/molecule)} \\ &= 6.2422 \times 10^{11} \text{ (eV/molecule)} \end{aligned}$$

$$\text{Avogadro number, } N_o = 6.025 \times 10^{23} \text{ (1/mole)}$$

$$1 \text{ (cal)} = 4.184 \text{ (joule)}$$

Figure 1-2 compares the order of energy expressed in terms of $\tilde{\nu}$ (cm^{-1}), λ (cm) and ν (Hz).

As indicated in Fig. 1-2 and Table 1-2, the magnitude of ΔE is different depending upon the origin of the transition. In this book, we are mainly concerned with vibrational transitions which are observed in infrared (IR) or Raman spectra**. These transitions appear in the $10^4 \sim 10^2 \text{ cm}^{-1}$ region and

*If a molecule loses ΔE via molecular collision, it is called a “radiationless transition.”

**Pure rotational and rotational–vibrational transitions are also observed in IR and Raman spectra. Many excellent textbooks are available on these and other subjects (see general references given at the end of this chapter).

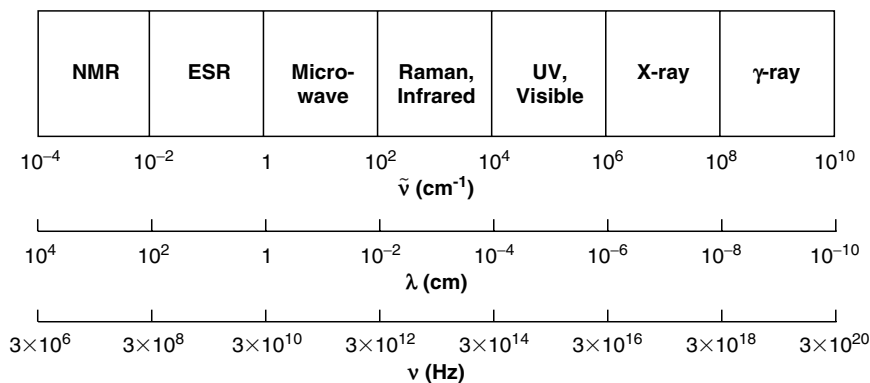


Figure 1-2 Energy units for various portions of electromagnetic spectrum.

Table 1-2 Spectral Regions and Their Origins

Spectroscopy	Range ($\tilde{\nu}$, cm^{-1})	Origin
γ -ray	$10^{10} - 10^8$	Rearrangement of elementary particles in the nucleus
X-ray (ESCA, PES)	$10^8 - 10^6$	Transitions between energy levels of inner electrons of atoms and molecules
UV-Visible	$10^6 - 10^4$	Transitions between energy levels of valence electrons of atoms and molecules
Raman and infrared	$10^4 - 10^2$	Transitions between vibrational levels (change of configuration)
Microwave	$10^2 - 1$	Transitions between rotational levels (change of orientation)
Electron spin resonance (ESR)	$1 - 10^{-2}$	Transitions between electron spin levels in magnetic field
Nuclear magnetic resonance (NMR)	$10^{-2} - 10^{-4}$	Transitions between nuclear spin levels in magnetic fields

originate from vibrations of nuclei constituting the molecule. As will be shown later, Raman spectra are intimately related to electronic transitions. Thus, it is important to know the relationship between electronic and vibrational states. On the other hand, vibrational spectra of small molecules in the gaseous state exhibit rotational fine structures.* Thus, it is also important to

*In solution, rotational fine structures are not observed because molecular collisions (10^{-13} s) occur before one rotation is completed (10^{-11} s) and the levels of individual molecules are perturbed differently. In the solid state, molecular rotation does not occur because of intermolecular interactions.

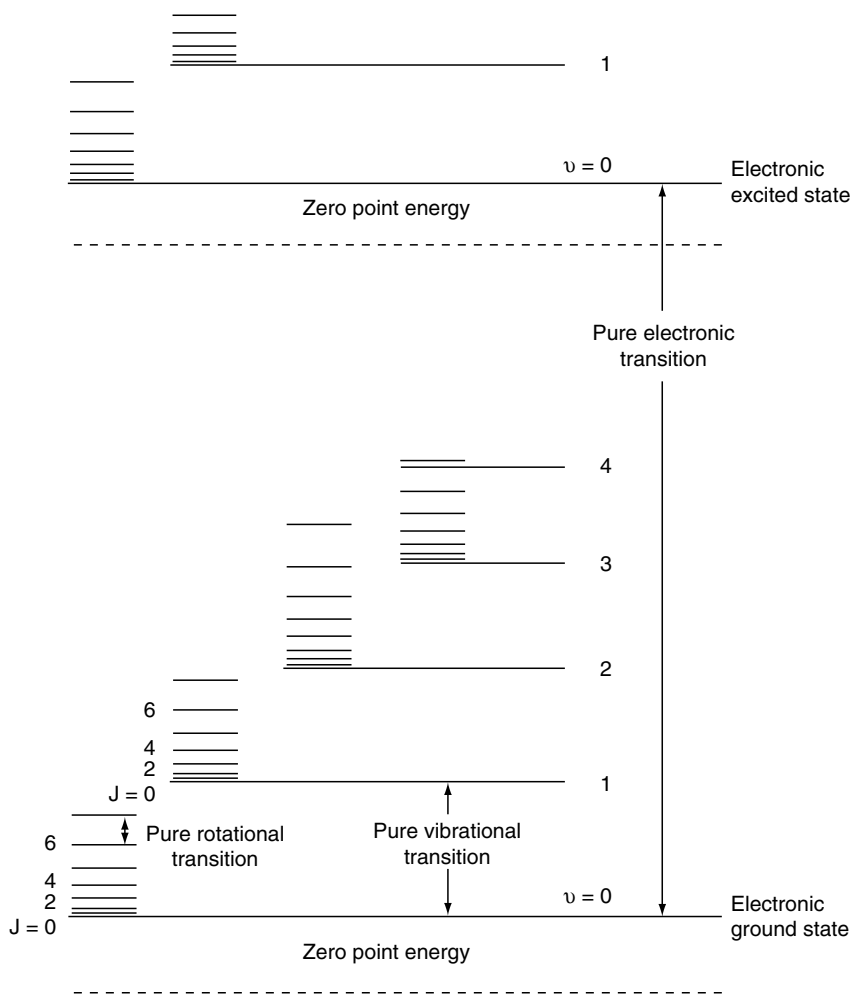
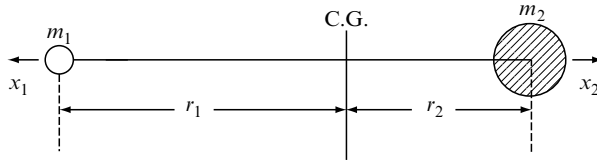


Figure 1-3 Energy levels of a diatomic molecule. (The actual spacings of electronic levels are much larger, and those of rotational levels much smaller, than those shown in the figure.)

know the relationship between vibrational and rotational states. Figure 1-3 illustrates the three types of transitions for a diatomic molecule.

1.3 Vibration of a Diatomic Molecule

Consider the vibration of a diatomic molecule in which two atoms are connected by a chemical bond.



Here, m_1 and m_2 are the masses of atom 1 and 2, respectively, and r_1 and r_2 are the distances from the center of gravity (C.G.) to the atoms designated. Thus, $r_1 + r_2$ is the equilibrium distance, and x_1 and x_2 are the displacements of atoms 1 and 2, respectively, from their equilibrium positions. Then, the conservation of the center of gravity requires the relationships:

$$m_1 r_1 = m_2 r_2, \quad (1-10)$$

$$m_1(r_1 + x_1) = m_2(r_2 + x_2). \quad (1-11)$$

Combining these two equations, we obtain

$$x_1 = \left(\frac{m_2}{m_1}\right)x_2 \quad \text{or} \quad x_2 = \left(\frac{m_1}{m_2}\right)x_1. \quad (1-12)$$

In the classical treatment, the chemical bond is regarded as a spring that obeys Hooke's law, where the restoring force, f , is expressed as

$$f = -K(x_1 + x_2). \quad (1-13)$$

Here K is the force constant, and the minus sign indicates that the directions of the force and the displacement are opposite to each other. From (1-12) and (1-13), we obtain

$$f = -K\left(\frac{m_1 + m_2}{m_1}\right)x_2 = -K\left(\frac{m_1 + m_2}{m_2}\right)x_1. \quad (1-14)$$

Newton's equation of motion ($f = ma$; $m = \text{mass}$; $a = \text{acceleration}$) is written for each atom as

$$m_1 \frac{d^2 x_1}{dt^2} = -K\left(\frac{m_1 + m_2}{m_2}\right)x_1, \quad (1-15)$$

$$m_2 \frac{d^2 x_2}{dt^2} = -K\left(\frac{m_1 + m_2}{m_1}\right)x_2. \quad (1-16)$$

By adding

$$(1-15) \times \left(\frac{m_2}{m_1 + m_2}\right) \quad \text{and} \quad (1-16) \times \left(\frac{m_1}{m_1 + m_2}\right),$$

we obtain

$$\frac{m_1 m_2}{m_1 + m_2} \left(\frac{d^2 x_1}{dt^2} + \frac{d^2 x_2}{dt^2} \right) = -K(x_1 + x_2). \quad (1-17)$$

Introducing the reduced mass (μ) and the displacement (q), (1-17) is written as

$$\mu \frac{d^2 q}{dt^2} = -Kq. \quad (1-18)$$

The solution of this differential equation is

$$q = q_0 \sin(2\pi\nu_0 t + \varphi), \quad (1-19)$$

where q_0 is the maximum displacement and φ is the phase constant, which depends on the initial conditions. ν_0 is the classical vibrational frequency given by

$$\nu_0 = \frac{1}{2\pi} \sqrt{\frac{K}{\mu}}. \quad (1-20)$$

The potential energy (V) is defined by

$$dV = -f dq = Kq dq.$$

Thus, it is given by

$$\begin{aligned} V &= \frac{1}{2} Kq^2 \\ &= \frac{1}{2} Kq_0^2 \sin^2(2\pi\nu_0 t + \varphi) \\ &= 2\pi^2 \nu_0^2 \mu q_0^2 \sin^2(2\pi\nu_0 t + \varphi). \end{aligned} \quad (1-21)$$

The kinetic energy (T) is

$$\begin{aligned} T &= \frac{1}{2} m_1 \left(\frac{dx_1}{dt} \right)^2 + \frac{1}{2} m_2 \left(\frac{dx_2}{dt} \right)^2 \\ &= \frac{1}{2} \mu \left(\frac{dq}{dt} \right)^2 \\ &= 2\pi^2 \nu_0^2 \mu q_0^2 \cos^2(2\pi\nu_0 t + \varphi). \end{aligned} \quad (1-22)$$

Thus, the total energy (E) is

$$\begin{aligned} E &= T + V \\ &= 2\pi^2 \nu_0^2 \mu q_0^2 = \text{constant} \end{aligned} \quad (1-23)$$

Figure 1-4 shows the plot of V as a function of q . This is a parabolic potential, $V = \frac{1}{2} Kq^2$, with $E = T$ at $q = 0$ and $E = V$ at $q = \pm q_0$. Such a vibrator is called a *harmonic oscillator*.

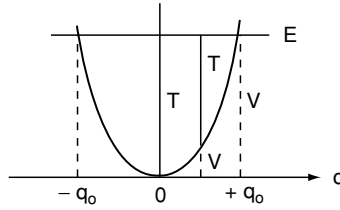


Figure 1-4 Potential energy diagram for a harmonic oscillator.

In quantum mechanics (18,19) the vibration of a diatomic molecule can be treated as a motion of a single particle having mass μ whose potential energy is expressed by (1-21). The Schrödinger equation for such a system is written as

$$\frac{d^2\psi}{dq^2} + \frac{8\pi^2\mu}{h^2} \left(E - \frac{1}{2}Kq^2 \right) \psi = 0. \quad (1-24)$$

If (1-24) is solved with the condition that ψ must be single-valued, finite and continuous, the eigenvalues are

$$E_v = hv \left(v + \frac{1}{2} \right) = hc\tilde{\nu} \left(v + \frac{1}{2} \right), \quad (1-25)$$

with the frequency of vibration

$$v = \frac{1}{2\pi} \sqrt{\frac{K}{\mu}} \quad \text{or} \quad \tilde{\nu} = \frac{1}{2\pi c} \sqrt{\frac{K}{\mu}}. \quad (1-26)$$

Here, v is the vibrational quantum number, and it can have the values 0, 1, 2, 3, ... The corresponding eigenfunctions are

$$\psi_v = \frac{(\alpha/\pi)^{1/4}}{\sqrt{2^v v!}} e^{-\alpha q^2/2} H_v(\sqrt{\alpha}q), \quad (1-27)$$

where

$$\alpha = 2\pi\sqrt{\mu K/h} = 4\pi^2\mu\nu/h \quad \text{and} \quad H_v(\sqrt{\alpha}q)$$

is a Hermite polynomial of the v th degree. Thus, the eigenvalues and the corresponding eigenfunctions are

$$\begin{aligned} v = 0, & \quad E_0 = \frac{1}{2}hv, & \psi_0 &= (\alpha/\pi)^{1/4} e^{-\alpha q^2/2} \\ v = 1, & \quad E_1 = \frac{3}{2}hv, & \psi_1 &= (\alpha/\pi)^{1/4} 2^{1/2} q e^{-\alpha q^2/2}. \\ & \vdots & & \vdots \end{aligned} \quad (1-28)$$

One should note that the quantum-mechanical frequency (1-26) is exactly the same as the classical frequency (1-20). However, several marked differences must be noted between the two treatments. First, classically, E is zero when q is zero. Quantum-mechanically, the lowest energy state ($v = 0$) has the energy of $\frac{1}{2}h\nu$ (zero point energy) (see Fig. 1-3) which results from Heisenberg's uncertainty principle. Secondly, the energy of a such a vibrator can change continuously in classical mechanics. In quantum mechanics, the energy can change only in units of $h\nu$. Thirdly, the vibration is confined within the parabola in classical mechanics since T becomes negative if $|q| > |q_0|$ (see Fig. 1-4). In quantum mechanics, the probability of finding q outside the parabola is not zero (tunnel effect) (Fig. 1-5).

In the case of a harmonic oscillator, the separation between the two successive vibrational levels is always the same ($h\nu$). This is not the case of an actual molecule whose potential is approximated by the Morse potential function shown by the solid curve in Fig. 1-6.

$$V = D_e(1 - e^{-\beta q})^2. \quad (1-29)$$

Here, D_e is the dissociation energy and β is a measure of the curvature at the bottom of the potential well. If the Schrödinger equation is solved with this potential, the eigenvalues are (18,19)

$$E_v = hc\omega_e\left(v + \frac{1}{2}\right) - hc\chi_e\omega_e\left(v + \frac{1}{2}\right)^2 + \dots, \quad (1-30)$$

where ω_e is the wavenumber corrected for anharmonicity, and $\chi_e\omega_e$ indicates the magnitude of anharmonicity. Equation (1-30) shows that the energy levels of the anharmonic oscillator are no longer equidistant, and the separation decreases with increasing v as shown in Fig. 1-6. Thus far, anharmonicity

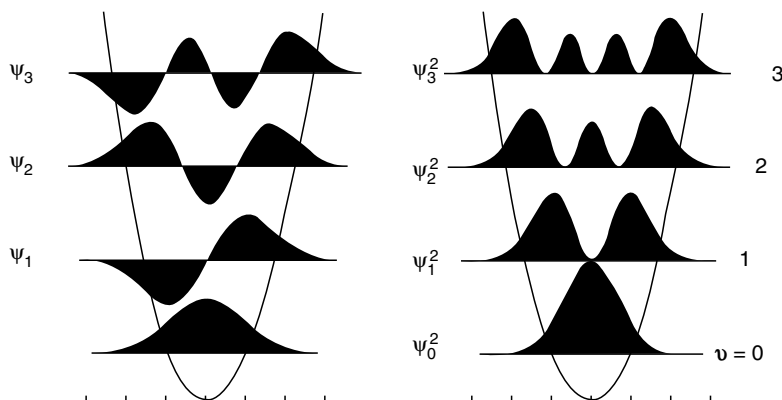


Figure 1-5 Wave functions (left) and probability distributions (right) of the harmonic oscillator.

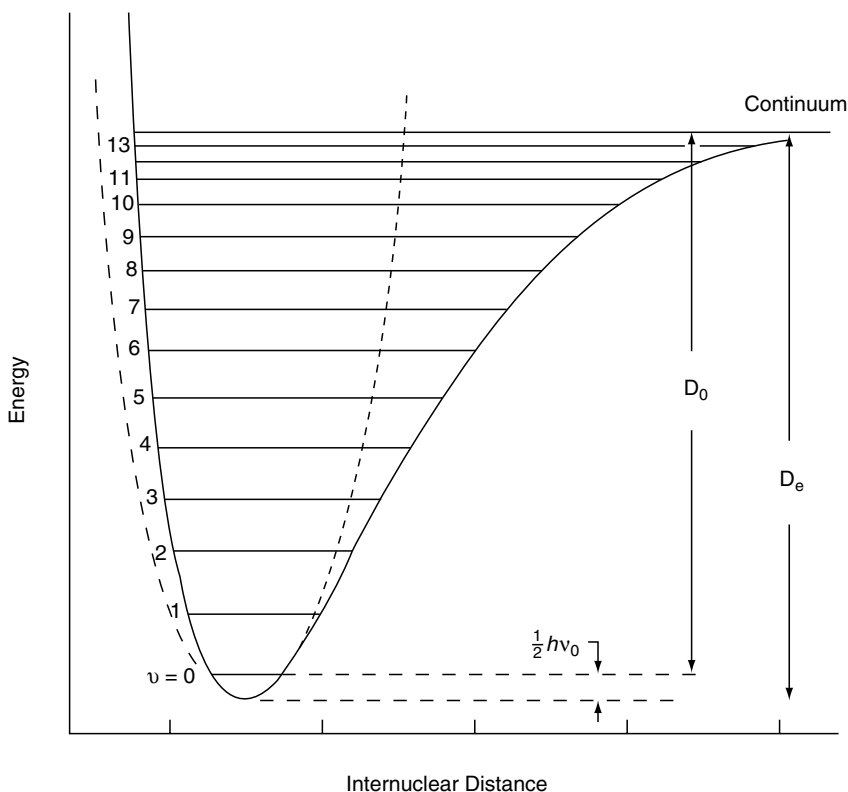


Figure 1-6 Potential energy curve for a diatomic molecule. Solid line indicates a Morse potential that approximates the actual potential. Broken line is a parabolic potential for a harmonic oscillator. D_e and D_0 are the theoretical and spectroscopic dissociation energies, respectively.

corrections have been made mostly on diatomic molecules (see Table 1-3), because of the complexity of calculations for large molecules.

According to quantum mechanics, only those transitions involving $\Delta v = \pm 1$ are allowed for a harmonic oscillator. If the vibration is anharmonic, however, transitions involving $\Delta v = \pm 2, \pm 3, \dots$ (overtones) are also weakly allowed by selection rules. Among many $\Delta v = \pm 1$ transitions, that of $v = 0 \leftrightarrow 1$ (fundamental) appears most strongly both in IR and Raman spectra. This is expected from the Maxwell-Boltzmann distribution law, which states that the population ratio of the $v = 1$ and $v = 0$ states is given by

$$\frac{P_{v=1}}{P_{v=0}} = e^{-\Delta E/kT}, \quad (1-31)$$

Table 1-3 Relationships among Vibrational Frequency, Reduced Mass and Force Constant

Molecule	Obs. $\tilde{\nu}$ (cm^{-1})	ω_e (cm^{-1})	μ (amu)	K ($\text{mdyn}/\text{\AA}$)
H ₂	4,160	4,395	0.5041	5.73
HD	3,632	3,817	0.6719	5.77
D ₂	2,994	3,118	1.0074	5.77
HF	3,962	4,139	0.9573	9.65
HCl	2,886	2,989	0.9799	5.16
HBr	2,558	2,650	0.9956	4.12
HI	2,233	2,310	1.002	3.12
F ₂	892	—	9.5023	4.45
Cl ₂	546	565	17.4814	3.19
Br ₂	319	323	39.958	2.46
I ₂	213	215	63.466	1.76
N ₂	2,331	2,360	7.004	22.9
CO	2,145	2,170	6.8584	19.0
NO	1,877	1,904	7.4688	15.8
O ₂	1,555	1,580	8.000	11.8

where ΔE is the energy difference between the two states, k is Boltzmann's constant (1.3807×10^{-16} erg/degree), and T is the absolute temperature. Since $\Delta E = hc\tilde{\nu}$, the ratio becomes smaller as $\tilde{\nu}$ becomes larger. At room temperature,

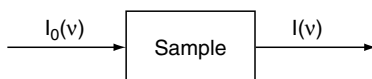
$$\begin{aligned}
 kT &= 1.38 \times 10^{-6} \text{ (erg/degree)} \times 300 \text{ (degree)} \\
 &= 4.14 \times 10^{-14} \text{ (erg)} \\
 &= [4.14 \times 10^{-14} \text{ (erg)}] / [1.99 \times 10^{-16} \text{ (erg/cm}^{-1}\text{)}] \\
 &= 208 \text{ (cm}^{-1}\text{)}.
 \end{aligned}$$

Thus, if $\tilde{\nu} = 4,160 \text{ cm}^{-1}$ (H₂ molecule), $P(v=1)/P(v=0) = 2.19 \times 10^{-9}$. Therefore, almost all of the molecules are at $v=0$. On the other hand, if $\tilde{\nu} = 213 \text{ cm}^{-1}$ (I₂ molecule), this ratio becomes 0.36. Thus, about 27% of the I₂ molecules are at $v=1$ state. In this case, the transition $v=1 \rightarrow 2$ should be observed on the low-frequency side of the fundamental with much less intensity. Such a transition is called a "hot band" since it tends to appear at higher temperatures.

1.4 Origin of Raman Spectra

As stated in Section 1.1, vibrational transitions can be observed in either IR or Raman spectra. In the former, we measure the absorption of infrared light by the sample as a function of frequency. The molecule absorbs $\Delta E = h\nu$ from

IR



Raman

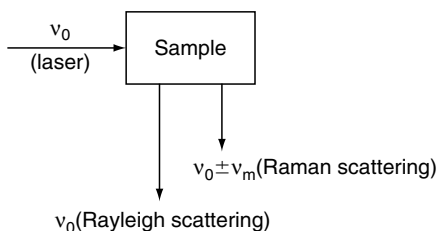


Figure 1-7 Differences in mechanism of Raman vs IR.

the IR source at each vibrational transition. The intensity of IR absorption is governed by the Beer–Lambert law:

$$I = I_0 e^{-\varepsilon cd}. \quad (1-32)$$

Here, I_0 and I denote the intensities of the incident and transmitted beams, respectively, ε is the molecular absorption coefficient,* and c and d are the concentration of the sample and the cell length, respectively (Fig. 1-7). In IR spectroscopy, it is customary to plot the percentage transmission (T) versus wave number ($\bar{\nu}$):

$$T(\%) = \frac{I}{I_0} \times 100. \quad (1-33)$$

It should be noted that T (%) is not proportional to c . For quantitative analysis, the absorbance (A) defined here should be used:

$$A = \log \frac{I_0}{I} = \varepsilon cd. \quad (1-34)$$

The origin of Raman spectra is markedly different from that of IR spectra. In Raman spectroscopy, the sample is irradiated by intense laser beams in the UV-visible region (ν_0), and the scattered light is usually observed in the direction perpendicular to the incident beam (Fig. 1-7; see also Chapter 2,

* ε has the dimension of $l/\text{moles cm}$ when c and d are expressed in units of moles/liter and centimeters, respectively.

Section 2.3). The scattered light consists of two types: one, called *Rayleigh scattering*, is strong and has the same frequency as the incident beam (ν_0), and the other, called *Raman scattering*, is very weak ($\sim 10^{-5}$ of the incident beam) and has frequencies $\nu_0 \pm \nu_m$, where ν_m is a vibrational frequency of a molecule. The $\nu_0 - \nu_m$ and $\nu_0 + \nu_m$ lines are called the *Stokes* and *anti-Stokes* lines, respectively. Thus, in Raman spectroscopy, we measure the vibrational frequency (ν_m) as a shift from the incident beam frequency (ν_0).^{*} In contrast to IR spectra, Raman spectra are measured in the UV-visible region where the excitation as well as Raman lines appear.

According to classical theory, Raman scattering can be explained as follows: The electric field strength (E), of the electromagnetic wave (laser beam) fluctuates with time (t) as shown by Eq. (1-1):

$$E = E_0 \cos 2\pi\nu_0 t, \quad (1-35)$$

where E_0 is the vibrational amplitude and ν_0 is the frequency of the laser. If a diatomic molecule is irradiated by this light, an electric dipole moment P is induced:

$$P = \alpha E = \alpha E_0 \cos 2\pi\nu_0 t. \quad (1-36)$$

Here, α is a proportionality constant and is called *polarizability*. If the molecule is vibrating with a frequency ν_m , the nuclear displacement q is written

$$q = q_0 \cos 2\pi\nu_m t, \quad (1-37)$$

where q_0 is the vibrational amplitude. For a small amplitude of vibration, α is a linear function of q . Thus, we can write

$$\alpha = \alpha_0 + \left(\frac{\partial \alpha}{\partial q} \right)_0 q_0 + \dots \quad (1-38)$$

Here, α_0 is the polarizability at the equilibrium position, and $(\partial\alpha/\partial q)_0$ is the rate of change of α with respect to the change in q , evaluated at the equilibrium position.

Combining (1-36) with (1-37) and (1-38), we obtain

$$\begin{aligned} P &= \alpha E_0 \cos 2\pi\nu_0 t \\ &= \alpha_0 E_0 \cos 2\pi\nu_0 t + \left(\frac{\partial \alpha}{\partial q} \right)_0 q_0 E_0 \cos 2\pi\nu_0 t \\ &= \alpha_0 E_0 \cos 2\pi\nu_0 t + \left(\frac{\partial \alpha}{\partial q} \right)_0 q_0 E_0 \cos 2\pi\nu_0 t \cos 2\pi\nu_m t \end{aligned}$$

^{*}Although Raman spectra are normally observed for vibrational and rotational transitions, it is possible to observe Raman spectra of electronic transitions between ground states and low-energy excited states.

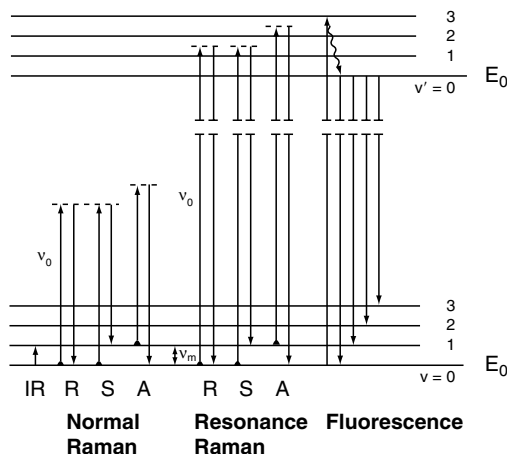


Figure 1-8 Comparison of energy levels for the normal Raman, resonance Raman, and fluorescence spectra.

$$= \alpha_0 E_0 \cos 2\pi\nu_0 t + \frac{1}{2} \left(\frac{\partial \alpha}{\partial q} \right)_0 q_0 E_0 [\cos \{2\pi(\nu_0 + \nu_m)t\} + \cos \{2\pi(\nu_0 - \nu_m)t\}]. \quad (1-39)$$

According to classical theory, the first term represents an oscillating dipole that radiates light of frequency ν_0 (Rayleigh scattering), while the second term corresponds to the Raman scattering of frequency $\nu_0 + \nu_m$ (anti-Stokes) and $\nu_0 - \nu_m$ (Stokes). If $(\partial\alpha/\partial q)_0$ is zero, the vibration is not Raman-active. Namely, to be Raman-active, the rate of change of polarizability (α) with the vibration must not be zero.

Figure 1-8 illustrates Raman scattering in terms of a simple diatomic energy level. In IR spectroscopy, we observe that $v = 0 \rightarrow 1$ transition at the electronic ground state. In normal Raman spectroscopy, the exciting line (ν_0) is chosen so that its energy is far below the first electronic excited state. The dotted line indicates a “virtual state” to distinguish it from the real excited state. As stated in Section 1.2, the population of molecules at $v = 0$ is much larger than that at $v = 1$ (Maxwell–Boltzmann distribution law). Thus, the Stokes (*S*) lines are stronger than the anti-Stokes (*A*) lines under normal conditions. Since both give the same information, it is customary to measure only the Stokes side of the spectrum. Figure 1-9 shows the Raman spectrum of CCl_4^* .

*A Raman spectrum is expressed as a plot, intensity vs. Raman shift ($\Delta\tilde{\nu} = \tilde{\nu}_0 \pm \tilde{\nu}$). However, $\Delta\tilde{\nu}$ is often written as $\tilde{\nu}$ for brevity.

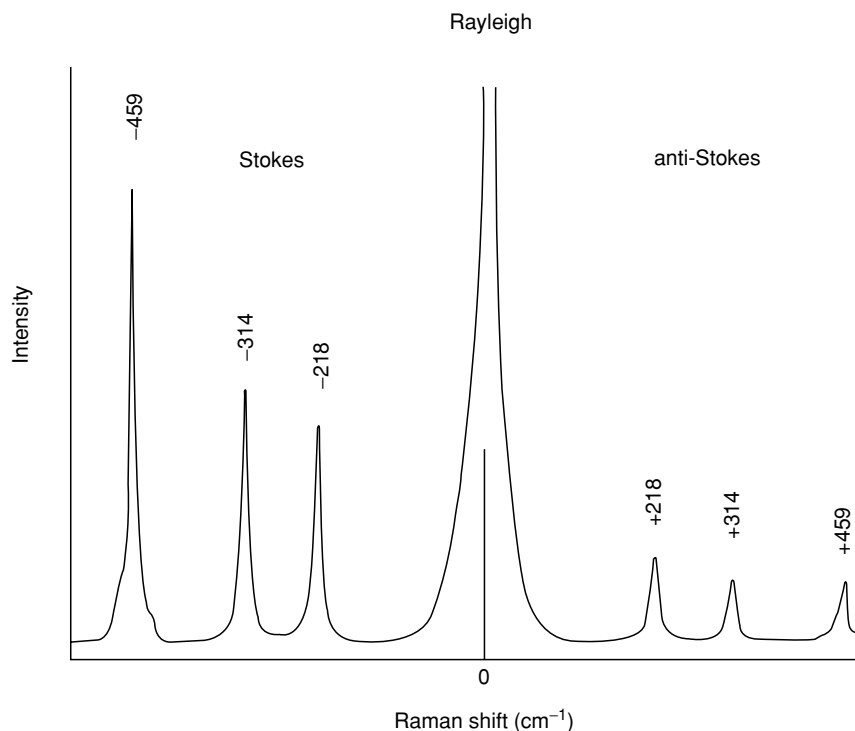


Figure 1-9 Raman spectrum of CCl₄ (488.0 nm excitation).

Resonance Raman (RR) scattering occurs when the exciting line is chosen so that its energy intercepts the manifold of an electronic excited state. In the liquid and solid states, vibrational levels are broadened to produce a continuum. In the gaseous state, a continuum exists above a series of discrete levels. Excitation of these continua produces RR spectra that show extremely strong enhancement of Raman bands originating in this particular electronic transition. Because of its importance, RR spectroscopy will be discussed in detail in Section 1.15. The term “pre-resonance” is used when the exciting line is close in energy to the electronic excited state. Resonance fluorescence (RF) occurs when the molecule is excited to a discrete level of the electronic excited state (20). This has been observed for gaseous molecules such as I_2 , Br_2 . Finally, fluorescence spectra are observed when the excited state molecule decays to the lowest vibrational level via radiationless transitions and then emits radiation, as shown in Fig. 1-8. The lifetime of the excited state in RR is very short ($\sim 10^{-14}$ s), while those in RF and fluorescence are much longer ($\sim 10^{-8}$ to 10^{-5} s).

1.5 Factors Determining Vibrational Frequencies

According to Eq. (1-26), the vibrational frequency of a diatomic molecule is given by

$$\tilde{\nu} = \frac{1}{2\pi c} \sqrt{\frac{K}{\mu}} \quad (1-40)$$

where K is the force constant and μ is the reduced mass. This equation shows that $\tilde{\nu}$ is proportional to \sqrt{K} (force constant effect), but inversely proportional to $\sqrt{\mu}$ (mass effect). To calculate the force constant, it is convenient to rewrite the preceding equations as

$$K = 4\pi^2 c^2 \omega_e^2 \mu. \quad (1-41)$$

Here, the vibrational frequency (observed) has been replaced by ω_e (Eq. (1-30)) in order to obtain a more accurate force constant. Using the unit of millidynes/Å (mdyn/Å) or 10^5 (dynes/cm) for K , and the atomic weight unit (awu) for μ , Eq. (1-41) can be written as

$$\begin{aligned} K &= 4(3.14)^2 (3 \times 10^{10})^2 \left[\frac{\mu}{6,025 \times 10^{23}} \right] \omega_e^2 \\ &= (5.8883 \times 10^{-2}) \mu \omega_e^2. \end{aligned} \quad (1-42)$$

For H^{35}Cl , $\omega_e = 2,989 \text{ cm}^{-1}$ and μ is 0.9799. Then, its K is 5.16×10^5 (dynes/cm) or 5.16 (mdyn/Å). If such a calculation is made for a number of diatomic molecules, we obtain the results shown in Table 1-3. In all four series of compounds, the frequency decreases in going downward in the table. However, the origin of this downward shift is different in each case. In the $\text{H}_2 > \text{HD} > \text{D}_2$ series, it is due to the mass effect since the force constant is not affected by isotopic substitution. In the $\text{HF} > \text{HCl} > \text{HBr} > \text{HI}$ series, it is due to the force constant effect (the bond becomes weaker in the same order) since the reduced mass is almost constant. In the $\text{F}_2 > \text{Cl}_2 > \text{Br}_2 > \text{I}_2$ series, however, both effects are operative; the molecule becomes heavier and the bond becomes weaker in the same order. Finally, in the $\text{N}_2 > \text{CO} > \text{NO} > \text{O}_2$, series, the decreasing frequency is due to the force constant effect that is expected from chemical formulas, such as $\text{N} \equiv \text{N}$, and $\text{O} = \text{O}$, with CO and NO between them.

It should be noted, however, that a large force constant does not necessarily mean a stronger bond, since the force constant is the curvature of the potential well near the equilibrium position,

$$K = \left(\frac{d^2 V}{dq^2} \right)_{q \rightarrow 0} \quad (1-43)$$

whereas the bond strength (dissociation energy) is measured by the depth of the potential well (Fig. 1-6). Thus, a large K means a sharp curvature near the bottom of the potential well, and does not directly imply a deep potential well. For example,

	HF	>	HCl	>	HBr	>	HI
K (mdyn/Å)	9.65		5.16		4.12		3.12
D_e (kcal/mole)	134.6		103.2		87.5		71.4

However,

	F ₂	>	Cl ₂	>	Br ₂	>	I ₂
K (mdyn/Å)	4.45		3.19		2.46		1.76
D_e (kcal/mole)	37.8	<	58.0	>	46.1	>	36.1

A rough parallel relationship is observed between the force constant and the dissociation energy when we plot these quantities for a large number of compounds.

1.6 Vibrations of Polyatomic Molecules

In diatomic molecules, the vibration occurs only along the chemical bond connecting the nuclei. In polyatomic molecules, the situation is complicated because all the nuclei perform their own harmonic oscillations. However, we can show that any of these complicated vibrations of a molecule can be expressed as a superposition of a number of "normal vibrations" that are completely independent of each other.

In order to visualize normal vibrations, let us consider a mechanical model of the CO₂ molecule shown in Fig. 1-10. Here, the C and O atoms are represented by three balls, weighing in proportion to their atomic weights, that are connected by springs of a proper strength in proportion to their force constants. Suppose that the C—O bonds are stretched and released

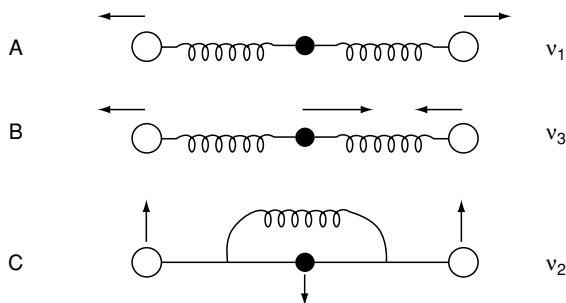


Figure 1-10 Atomic motions in normal modes of vibrations in CO₂.

simultaneously as shown in Fig. 1-10A. Then, the balls move back and forth along the bond direction. This is one of the normal vibrations of this model and is called the symmetric (in-phase) stretching vibration. In the real CO_2 molecule, its frequency (ν_1) is ca. $1,340\text{ cm}^{-1}$. Next, we stretch one C—O bond and shrink the other, and release all the balls simultaneously (Fig. 1-10B). This is another normal vibration and is called the antisymmetric (out-of-phase) stretching vibration. In the CO_2 molecule, its frequency (ν_3) is ca. $2,350\text{ cm}^{-1}$. Finally, we consider the case where the three balls are moved in the perpendicular direction and released simultaneously (Fig. 1-10C). This is the third type of normal vibration called the (symmetric) bending vibration. In the CO_2 molecule, its frequency (ν_2) is ca. 667 cm^{-1} .

Suppose that we strike this mechanical model with a hammer. Then, this model would perform an extremely complicated motion that has no similarity to the normal vibrations just mentioned. However, if this complicated motion is photographed with a stroboscopic camera with its frequency adjusted to that of the normal vibration, we would see that each normal vibration shown in Fig. 1-10 is performed faithfully. In real cases, the stroboscopic camera is replaced by an IR or Raman instrument that detects only the normal vibrations.

Since each atom can move in three directions (x, y, z), an N -atom molecule has $3N$ degrees of freedom of motion. However, the $3N$ includes six degrees of freedom originating from translational motions of the whole molecule in the three directions and rotational motions of the whole molecule about the three principal axes of rotation, which go through the center of gravity. Thus, the net vibrational degrees of freedom (number of normal vibrations) is $3N - 6$. In the case of linear molecules, it becomes $3N - 5$ since the rotation about the molecular axis does not exist. In the case of the CO_2 molecule, we have $3 \times 3 - 5 = 4$ normal vibrations shown in Fig. 1-11. It should be noted that ν_{2a} and ν_{2b} have the same frequency and are different only in the direction of vibration by 90° . Such a pair is called a set of doubly degenerate vibrations. Only two such vibrations are regarded as unique since similar vibrations in any other directions can be expressed as a linear combination of ν_{2a} and ν_{2b} . Figure 1-12 illustrates the three normal vibrations ($3 \times 3 - 6 = 3$) of the H_2O molecule.

Theoretical treatments of normal vibrations will be described in Section 1.20. Here, it is sufficient to say that we designate “normal coordinates” Q_1, Q_2 and Q_3 for the normal vibrations such as the ν_1, ν_2 and ν_3 , respectively, of Fig. 1-12, and that the relationship between a set of normal coordinates and a set of Cartesian coordinates (q_1, q_2, \dots) is given by

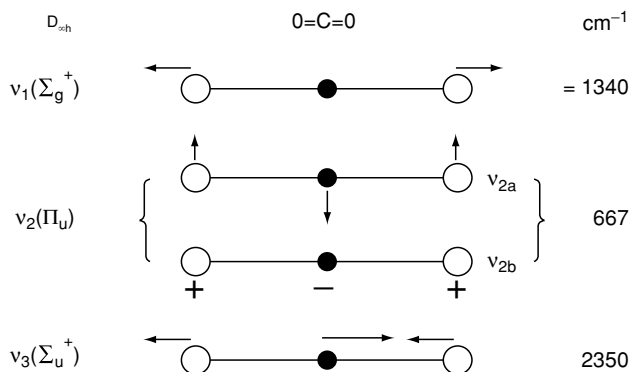


Figure 1-11 Normal modes of vibration in CO_2 (+ and - denote vibrations going upward and downward, respectively, in direction perpendicular to the paper plane).

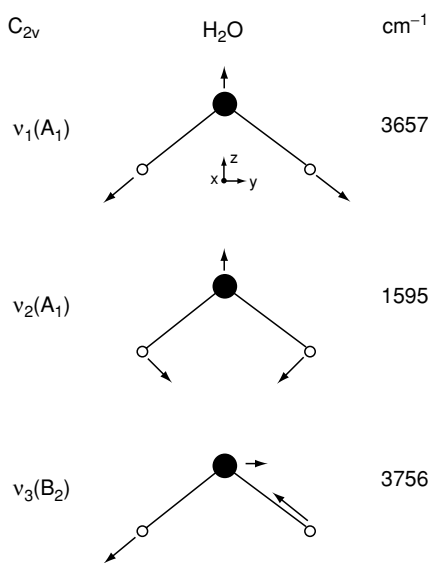


Figure 1-12 Normal modes of vibrations in H_2O .

$$\begin{aligned}
 q_1 &= B_{11}Q_1 + B_{12}Q_2 + \dots, \\
 q_2 &= B_{21}Q_1 + B_{22}Q_2 + \dots, \\
 &\dots,
 \end{aligned}
 \tag{1-44}$$

so that the modes of normal vibrations can be expressed in terms of Cartesian coordinates if the B_{ij} terms are calculated.

1.7 Selection Rules for Infrared and Raman Spectra

To determine whether the vibration is active in the IR and Raman spectra, the selection rules must be applied to each normal vibration. Since the origins of IR and Raman spectra are markedly different (Section 1.4), their selection rules are also distinctively different. According to quantum mechanics (18,19) a vibration is IR-active if the dipole moment is changed during the vibration and is Raman-active if the polarizability is changed during the vibration.

The IR activity of small molecules can be determined by inspection of the mode of a normal vibration (normal mode). Obviously, the vibration of a homopolar diatomic molecule is not IR-active, whereas that of a heteropolar diatomic molecule is IR-active. As shown in Fig. 1-13, the dipole moment of the H_2O molecule is changed during each normal vibration. Thus, all these vibrations are IR-active. From inspection of Fig. 1-11, one can readily see that ν_2 and ν_3 of the CO_2 molecule are IR-active, whereas ν_1 is not IR-active.

To discuss Raman activity, let us consider the nature of the polarizability (α) introduced in Section 1.4. When a molecule is placed in an electric field (laser beam), it suffers distortion since the positively charged nuclei are attracted toward the negative pole, and electrons toward the positive pole (Fig. 1-14). This charge separation produces an induced dipole moment (P) given by

$$P = \alpha E. \quad (1-45)^*$$

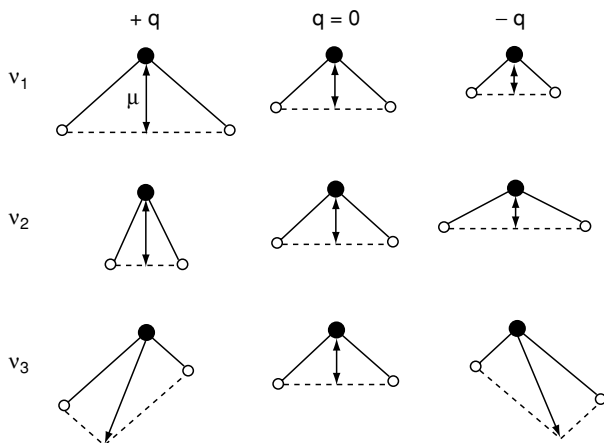


Figure 1-13 Change in dipole moment for H_2O molecule during each normal vibration.

*A more accurate expression is given by Eq. 3-1 in Chapter 3.

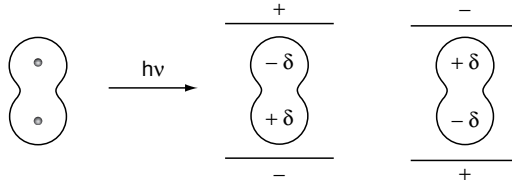


Figure 1-14 Polarization of a diatomic molecule in an electric field.

In actual molecules, such a simple relationship does not hold since both P and E are vectors consisting of three components in the x , y and z directions. Thus, Eq. (1-45) must be written as

$$\begin{aligned} P_x &= \alpha_{xx}E_x + \alpha_{xy}E_y + \alpha_{xz}E_z, \\ P_y &= \alpha_{yx}E_x + \alpha_{yy}E_y + \alpha_{yz}E_z, \\ P_z &= \alpha_{zx}E_x + \alpha_{zy}E_y + \alpha_{zz}E_z. \end{aligned} \quad (1-46)$$

In matrix form, this is written as

$$\begin{bmatrix} P_x \\ P_y \\ P_z \end{bmatrix} = \begin{bmatrix} \alpha_{xx} & \alpha_{xy} & \alpha_{xz} \\ \alpha_{yx} & \alpha_{yy} & \alpha_{yz} \\ \alpha_{zx} & \alpha_{zy} & \alpha_{zz} \end{bmatrix} \begin{bmatrix} E_x \\ E_y \\ E_z \end{bmatrix} \quad (1-47)$$

The first matrix on the right-hand side is called the *polarizability tensor*. In normal Raman scattering, this tensor is symmetric; $\alpha_{xy} = \alpha_{yz}$, $\alpha_{xz} = \alpha_{zx}$ and $\alpha_{yz} = \alpha_{zy}$. According to quantum mechanics, the vibration is Raman-active if one of these components of the polarizability tensor is changed during the vibration.

In the case of small molecules, it is easy to see whether or not the polarizability changes during the vibration. Consider diatomic molecules such as H_2 or linear molecules such as CO_2 . Their electron clouds have an elongated water melon like shape with circular cross-sections. In these molecules, the electrons are more polarizable (a larger α) along the chemical bond than in the direction perpendicular to it. If we plot α_i (α in the i -direction) from the center of gravity in all directions, we end up with a three-dimensional surface. Conventionally, we plot $1/\sqrt{\alpha_i}$ rather than α_i itself and call the resulting three-dimensional body a *polarizability ellipsoid*. Figure 1-15 shows the changes of such an ellipsoid during the vibrations of the CO_2 molecule.

In terms of the polarizability ellipsoid, the vibration is Raman-active if the *size*, *shape* or *orientation* changes during the normal vibration. In the ν_1 vibration, the size of the ellipsoid is changing; the diagonal elements (α_{xx} , α_{yy} and α_{zz}) are changing simultaneously. Thus, it is Raman-active. Although the size of the ellipsoid is changing during the ν_3 vibration, the ellipsoids at

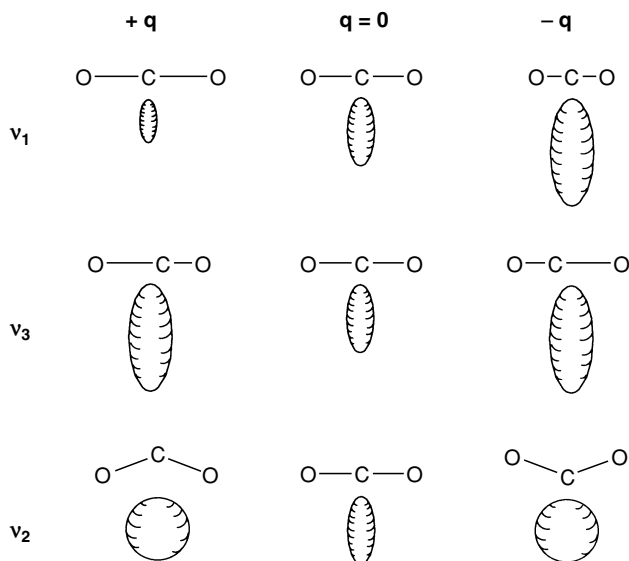


Figure 1-15 Changes in polarizability ellipsoids during vibration of CO_2 molecule.

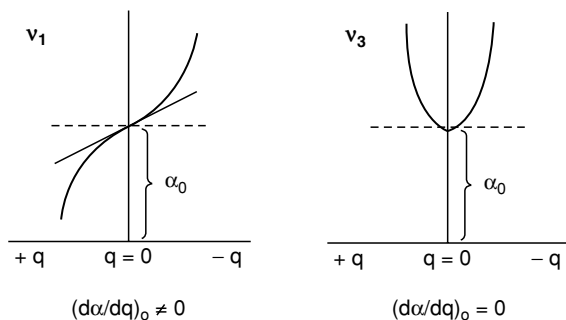


Figure 1-16 Difference between v_1 and v_3 vibrations in CO_2 molecule.

two extreme displacements ($+q$ and $-q$) are exactly the same in this case. Thus, this vibration is not Raman-active if we consider a small displacement. The difference between the v_1 and v_3 is shown in Fig. 1-16. Note that the Raman activity is determined by $(d\alpha/dq)_0$ (slope near the equilibrium position). During the v_2 vibration, the shape of the ellipsoid is sphere-like at two extreme configurations. However, the size and shape of the ellipsoid are exactly the same at $+q$ and $-q$. Thus, it is not Raman-active for the same reason as that of v_3 . As these examples show, it is not necessary to figure out the exact size, shape or orientation of the ellipsoid to determine Raman activity.

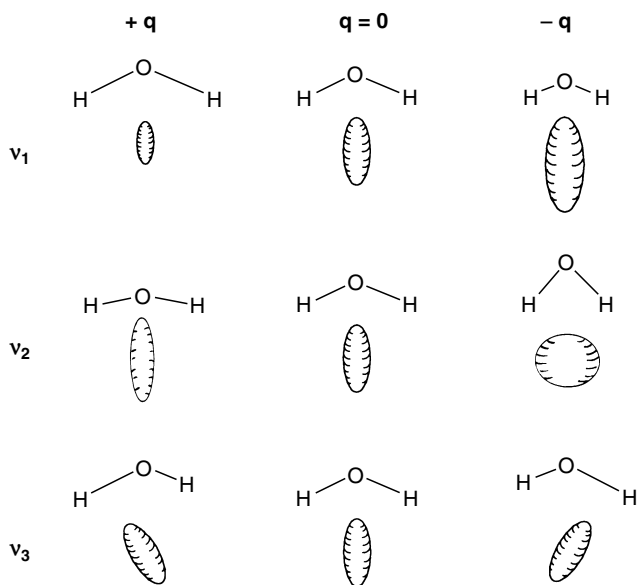


Figure 1-17 Changes in polarizability ellipsoid during normal vibrations of H_2O molecule.

Figure 1-17 illustrates the changes in the polarizability ellipsoid during the normal vibrations of the H_2O molecule. Its ν_1 vibration is Raman-active, as is the ν_1 vibration of CO_2 . The ν_2 vibration is also Raman-active because the *shape* of the ellipsoid is different at $+q$ and $-q$. In terms of the polarizability tensor, α_{xx} , α_{yy} and α_{zz} are all changing with different rates. Finally, the ν_3 vibration is Raman-active because the *orientation* of the ellipsoid is changing during the vibration. This activity occurs because an off-diagonal element (α_{yz} in this case) is changing.

One should note that, in CO_2 , the vibration that is symmetric with respect to the center of symmetry (ν_1) is Raman-active but not IR-active, whereas those that are antisymmetric with respect to the center of symmetry (ν_2 and ν_3) are IR-active but not Raman-active. This condition is called the *mutual exclusion principle* and holds for any molecules having a center of symmetry.*

The preceding examples demonstrate that IR and Raman activities can be determined by inspection of the normal mode. Clearly, such a simple approach is not applicable to large and complex molecules. As will be shown in Section 1.14, group theory provides elegant methods to determine IR and Raman activities of normal vibrations of such molecules.

*This principle holds even if a molecule has no atom at the center of symmetry (e.g., benzene).

1.8 Raman versus Infrared Spectroscopy

Although IR and Raman spectroscopies are similar in that both techniques provide information on vibrational frequencies, there are many advantages and disadvantages unique to each spectroscopy. Some of these are listed here.

1. As stated in Section 1.7, selection rules are markedly different between IR and Raman spectroscopies. Thus, some vibrations are only Raman-active while others are only IR-active. Typical examples are found in molecules having a center of symmetry for which the mutual exclusion rule holds. In general, a vibration is IR-active, Raman-active, or active in both; however, totally symmetric vibrations are always Raman-active.

2. Some vibrations are inherently weak in IR and strong in Raman spectra. Examples are the stretching vibrations of the $C\equiv C$, $C=C$, $P=S$, $S-S$ and $C-S$ bonds. In general, vibrations are strong in Raman if the bond is covalent, and strong in IR if the bond is ionic ($O-H$, $N-H$). For covalent bonds, the ratio of relative intensities of the $C\equiv C$, $C=C$ and $C-C$ bond stretching vibrations in Raman spectra is about 3:2:1.* Bending vibrations are generally weaker than stretching vibrations in Raman spectra.

3. Measurements of depolarization ratios provide reliable information about the symmetry of a normal vibration in solution (Section 1.9). Such information can not be obtained from IR spectra of solutions where molecules are randomly orientated.

4. Using the resonance Raman effect (Section 1.15), it is possible to selectively enhance vibrations of a particular chromophoric group in the molecule. This is particularly advantageous in vibrational studies of large biological molecules containing chromophoric groups (Sections 4.1 and 6.1.)

5. Since the diameter of the laser beam is normally 1–2 mm, only a small sample area is needed to obtain Raman spectra. This is a great advantage over conventional IR spectroscopy when only a small quantity of the sample (such as isotopic chemicals) is available.

6. Since water is a weak Raman scatterer, Raman spectra of samples in aqueous solution can be obtained without major interference from water vibrations. Thus, Raman spectroscopy is ideal for the studies of biological compounds in aqueous solution. In contrast, IR spectroscopy suffers from the strong absorption of water.

*In general, the intensity of Raman scattering increases as the $(d\alpha/dq)_0$ becomes larger.

7. Raman spectra of hygroscopic and/or air-sensitive compounds can be obtained by placing the sample in sealed glass tubing. In IR spectroscopy, this is not possible since glass tubing absorbs IR radiation.

8. In Raman spectroscopy, the region from 4,000 to 50 cm^{-1} can be covered by a single recording. In contrast, gratings, beam splitters, filters and detectors must be changed to cover the same region by IR spectroscopy.

Some disadvantages of Raman spectroscopy are the following:

1. A laser source is needed to observe weak Raman scattering. This may cause local heating and/or photodecomposition, especially in resonance Raman studies (Section 1.15) where the laser frequency is deliberately tuned in the absorption band of the molecule.
2. Some compounds fluoresce when irradiated by the laser beam.
3. It is more difficult to obtain rotational and rotation–vibration spectra with high resolution in Raman than in IR spectroscopy. This is because Raman spectra are observed in the UV-visible region where high resolving power is difficult to obtain.
4. The state of the art Raman system costs much more than a conventional FT-IR spectrophotometer although less expensive versions have appeared which are smaller and portable and suitable for process applications (Section 2-10).

Finally, it should be noted that vibrational (both IR and Raman) spectroscopy is unique in that it is applicable to the solid state as well as to the gaseous state and solution. In contrast, X-ray diffraction is applicable only to the crystalline state, whereas NMR spectroscopy is applicable largely to the sample in solution.

1.9 Depolarization Ratios

As stated in the preceding section, depolarization ratios of Raman bands provide valuable information about the symmetry of a vibration that is indispensable in making band assignments. Figure 1-18 shows a coordinate system which is used for measurements of depolarization ratios. A molecule situated at the origin is irradiated from the y -direction with plane polarized light whose electric vector oscillates on the yz -plane (E_z). If one observes scattered radiation from the x -direction, and measures the intensities in the

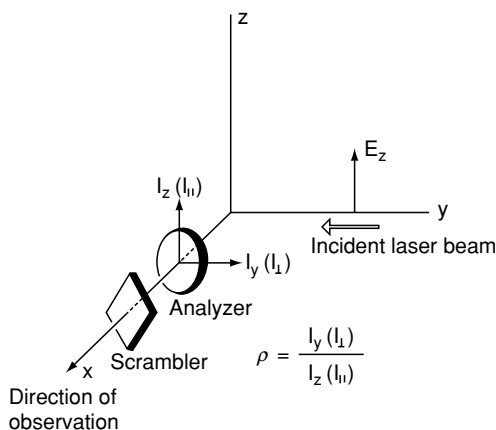


Figure 1-18 Irradiation of sample from the y -direction with plane polarized light, with the electronic vector in the z -direction.

$y(I_y)$ and $z(I_z)$ -directions using an analyzer, the depolarization ratio (ρ_p) measured by polarized light (p) is defined by

$$\rho_p = \frac{I_{\perp}(I_y)}{I_{\parallel}(I_z)}. \quad (1-48)$$

Figure 2-1 of Chapter 2 shows an experimental configuration for depolarization measurements in 90° scattering geometry. In this case, the polarizer is not used because the incident laser beam is almost completely polarized in the z direction. If a premonochromator is placed in front of the laser, a polarizer must be inserted to ensure complete polarization. The scrambler (crystal quartz wedge) must always be placed after the analyzer since the monochromator gratings show different efficiencies for \perp and \parallel polarized light. For information on precise measurements of depolarization ratios, see Refs. 21–24.

Suppose that a tetrahedral molecule such as CCl_4 is irradiated by plane polarized light (E_z). Then, the induced dipole (Section 1.7) also oscillates in the same yz -plane. If the molecule is performing the totally symmetric vibration, the polarizability ellipsoid is always sphere-like; namely, the molecule is polarized equally in every direction. Under such a circumstance, $I_{\perp}(I_y) = 0$ since the oscillating dipole emitting the radiation is confined to the xz -plane. Thus, $\rho_p = 0$. Such a vibration is called *polarized* (abbreviated as p). In liquids and solutions, molecules take random orientations. Yet this conclusion holds since the polarizability ellipsoid is spherical throughout the totally symmetric vibration.

If the molecule is performing a non-totally symmetric vibration, the polarizability ellipsoid changes its shape from a sphere to an ellipsoid during the

vibration. Then, the induced dipole would be largest along the direction of largest polarizability, namely along one of the minor axes of the ellipsoid. Since these axes would be randomly oriented in liquids and solutions, the induced dipole moments would also be randomly oriented. In this case, the ρ_p is nonzero, and the vibration is called *depolarized* (abbreviated as *dp*). Theoretically, we can show (25) that

$$\rho_p = \frac{3g^s + 5g^a}{10g^0 + 4g^s} \quad (1-49)$$

where

$$\begin{aligned} g^0 &= \frac{1}{3} (\alpha_{xx} + \alpha_{yy} + \alpha_{zz})^2, \\ g^s &= \frac{1}{3} [(\alpha_{xx} - \alpha_{yy})^2 + (\alpha_{yy} - \alpha_{zz})^2 + (\alpha_{zz} - \alpha_{xx})^2] \\ &\quad + \frac{1}{2} [(\alpha_{xy} + \alpha_{yx})^2 + (\alpha_{yz} + \alpha_{zy})^2 + (\alpha_{xz} + \alpha_{zx})^2], \\ g^a &= \frac{1}{2} [(\alpha_{xy} - \alpha_{yx})^2 + (\alpha_{xz} - \alpha_{zx})^2 + (\alpha_{yz} - \alpha_{zy})^2]. \end{aligned}$$

In normal Raman scattering, $g^a = 0$ since the polarizability tensor is symmetric. Then, (1-49) becomes

$$\rho_p = \frac{3g^s}{10g^0 + 4g^s} \quad (1-50)$$

For totally symmetric vibrations, $g^0 > 0$ and $g^s \geq 0$. Thus, $0 \leq \rho_p < \frac{3}{4}$ (polarized). For non-totally symmetric vibrations, $g^0 = 0$ and $g^s > 0$. Then, $\rho_p = \frac{3}{4}$ (depolarized).

In resonance Raman scattering ($g^a \neq 0$), it is possible to have $\rho_p > \frac{3}{4}$. For example, if $\alpha_{xy} = -\alpha_{yx}$ and the remaining off-diagonal elements are zero, $g^0 = g^s = 0$ and $g^a \neq 0$. Then, (1-49) gives $\rho_p \rightarrow \infty$. This is called *anomalous* (or *inverse*) *polarization* (abbreviated as *ap* or *ip*). As will be shown in Section 1.15, resonance Raman spectra of metalloporphyrins exhibit polarized (A_{1g}) and depolarized (B_{1g} and B_{2g}) vibrations as well as those of anomalous (or inverse) polarization (A_{2g}).

Figure 1-19 shows the Raman spectra of CCl_4 obtained with 90° scattering geometry. In this case, the ρ_p values obtained were 0.02 for the totally symmetric (459 cm^{-1}) and 0.75 for the non-totally symmetric modes (314 and 218 cm^{-1}). For ρ_p values in other scattering geometry, see Ref. 26.

Although polarization data are normally obtained for liquids and single crystals,* it is possible to measure depolarization ratios of Raman lines from solids by suspending them in a material with similar index of refraction (27).

*For an example of the use of polarized Raman spectra of calcite single crystal, see Section 1.19.

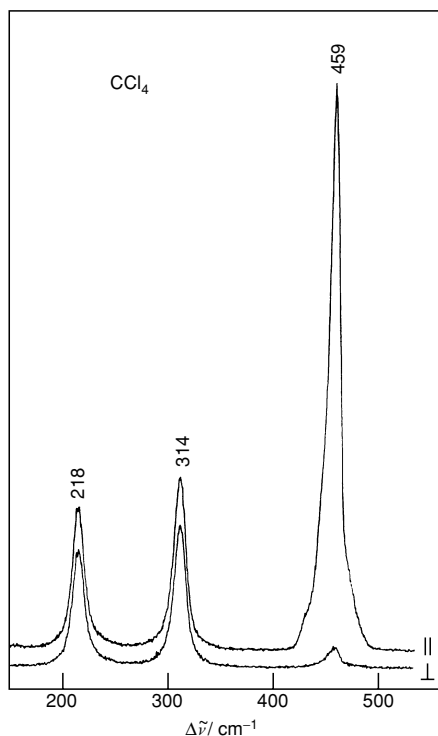


Figure 1-19 Raman spectrum of CCl_4 ($500\text{--}200\text{ cm}^{-1}$) in parallel and perpendicular polarization (488 nm excitation).

The use of suspensions can be circumvented by adding carbon black or CuO (28). The function of dark (black) additives appears to be related to a reduction of the penetration depth of the laser beam, causing an attenuation of reflected or refractive radiation, which is scrambled relative to polarization.

1.10 The Concept of Symmetry

The various experimental tools that are utilized today to solve structural problems in chemistry, such as Raman, infrared, NMR, magnetic measurements and the diffraction methods (electron, X-ray, and neutron), are based on symmetry considerations. Consequently, the symmetry concept as applied to molecules is thus very important.

Symmetry may be defined in a nonmathematical sense, where it is associated with beauty—with pleasing proportions or regularity in form, harmonious arrangement, or a regular repetition of certain characteristics (e.g.,